

USING THE EDDY-CURRENT METHOD TO MEASURE THE  
TEMPERATURE DEPENDENT RESISTIVITY IN METALS

by

Justin Sousa

A senior thesis submitted to the faculty of

Ithaca College

in partial fulfillment of the requirements for the degree of

Bachelor of Science

Department of Physics

Ithaca College

May 2009

Copyright © 2009 Justin Sousa

All Rights Reserved

ITHACA COLLEGE

DEPARTMENT APPROVAL

of a senior thesis submitted by

Justin Sousa

This thesis has been reviewed by the research advisor, senior thesis instructor,  
and department chair and has been found to be satisfactory.

---

Date

---

Bruce Thompson, Advisor

---

Date

---

Luke Keller, Senior Thesis Instructor

---

Date

---

Bruce Thompson, Chair

## ABSTRACT

### USING THE EDDY-CURRENT METHOD TO MEASURE THE TEMPERATURE DEPENDENT RESISTIVITY IN METALS

Justin Sousa

Department of Physics

Bachelor of Science

We use the eddy current method to measure the temperature dependence of resistivity for cylindrical rods of copper and aluminum. This method involves placing the samples inside a solenoid to immerse them in a magnetic field. Once the field has penetrated the conductor, we quickly remove the magnetic field by turning off the solenoid with a transistor. This abrupt change in magnetic flux through the material causes eddy currents to flow. These currents decay due to the resistivity of the material and create their own changing magnetic field. The decrease in magnetic flux due to the decaying eddy currents induces a voltage in a pickup coil surrounding the samples. A measurement of the electrical resistivity can be extracted from this voltage. We use a digital oscilloscope to transfer the signal to a computer for analysis. We performed the experiment with 1/2" diameter rods down to the boiling point of Nitrogen and with rods of various diameters at room temperature.

## ACKNOWLEDGMENTS

The first person I must thank is Professor Bruce Thompson for his guidance throughout the completion of this project. Professor Thompson's knowledge of physics and expertise in teaching as well as his friendship were an invaluable resource to me during this past year. Ron Gilmour, the Ithaca College science librarian, was also of great assistance and saved me many hours of searching for literature. I must also thank Professor Matthew C. Sullivan for guiding me throughout my last two years at Ithaca College. Over the past two years, Professor Sullivan has not only been a great friend, but has exhibited to me the traits necessary to be successful in physics and in life, and I owe a good majority of my knowledge of experimental physics to him. The entire physics department including Professors Michael 'Bodhi' Rogers, Luke Keller, and Daniel Briotta have also been of such great assistance during the past four years. The countless hours all of these physicists have dedicated to helping me over the past four years, whether in the form of lessons taught in classes or conversations outside of the classroom, have set me up for success in whatever I may decide to do. I can graduate knowing that the decision to study physics at Ithaca College has been one of best I have made in my life. I must also thank my parents for supporting me over the past twenty-one years of my life. It is by virtue of their hard work and intelligence that I am where I am today.



# Contents

<b>Table of Contents</b>	<b>vii</b>
<b>List of Figures</b>	<b>ix</b>
<b>1 Introduction</b>	<b>1</b>
<b>2 Experiment</b>	<b>7</b>
2.1 Theory . . . . .	7
2.2 Construction of Apparatus . . . . .	13
2.2.1 Adapted for Temperature-Dependent Measurements . . . . .	15
2.3 Data Acquisition . . . . .	16
<b>3 Results</b>	<b>23</b>
<b>4 Future Work</b>	<b>29</b>
<b>Bibliography</b>	<b>31</b>



# List of Figures

1.1	Temperature dependence of resistivity. . . . .	6
2.1	Coil signal vs. time . . . . .	12
2.2	A diagram showing the setup of our experiment . . . . .	18
2.3	A diagram of the electronic circuit . . . . .	19
2.4	LC oscillations for pickup coil . . . . .	20
2.5	Setup of silicon diode thermometers . . . . .	21
2.6	Temperature vs. time for warmup . . . . .	22
3.1	The temperature dependence of resistivity for copper . . . . .	26
3.2	The temperature dependence of resistivity for aluminum . . . . .	27



# Chapter 1

## Introduction

The concept of resistivity was first proposed by Georg Simon Ohm in 1826. Ohm discovered that, for certain materials, an applied electric field forced a current to flow. The ratio of the electric field to the current density is an intrinsic property of the material known as the resistivity,  $\rho$ .

$$\rho = \frac{\vec{E}}{\vec{j}} \quad (1.1)$$

Materials that have low resistivity, on the order of  $10^{-8} \Omega \cdot m$ , are called conductors. Likewise, materials that have high resistivity, on the order of  $10^{14} \Omega \cdot m$ , are called insulators. Semiconductors are materials with values of resistivity somewhere between that of conductors and insulators. These materials have certain properties that can be manipulated in useful ways by changing their temperature or by adding chemical impurities.

In 1900, Paul Drude developed the free electron model to mathematically express the origin of resistivity. The Drude Model considers the valence electrons to be free from the positively charged nuclei and allows them to accelerate in response to an electric field. However, collisions with the lattice ions slow the electrons and impart energy to the material. This energy exhibits itself as heating in the material and

is known as Joule heating. These collisions are represented as a drag force in the equation of motion for the electrons,

$$m \frac{d\vec{v}}{dt} = e\vec{E} - \frac{m\vec{v}}{\tau}, \quad (1.2)$$

where  $\tau$  is the time between collisions with the lattice,  $m$  is the mass of the electron, and  $\vec{v}$  is the velocity. The steady state solution to this equation, known as the drift velocity, is the average velocity of the electrons in the direction opposite the applied field.

$$\langle \vec{v}_d \rangle = -\frac{e\tau}{m} \vec{E} \quad (1.3)$$

The drift velocity determines the current density,

$$\vec{j} = n(-e)\langle \vec{v}_d \rangle = \frac{ne^2\tau}{m} \vec{E}, \quad (1.4)$$

where  $n$  is the volume density of electrons. Substituting Eqn.(1.4) into Eqn.(1.1) and solving for the ratio of  $E$  over  $j$ , we get the Drude form of resistivity,

$$\rho = \frac{m}{ne^2\tau}. \quad (1.5)$$

The Drude model offers theoretical justifications for some of the experimentally determined transport properties of electrons in solids. Unfortunately, it fails to correctly predict fundamental properties such as the temperature dependence of resistivity and the specific heat of a material.

With the advent of quantum mechanics in the early twentieth century, it became clear to physicists that a new model was necessary to explain the transport properties of electrons in solids. This new model was developed by Arnold Sommerfeld and Hans Bethe in 1933. The Quantum Mechanical Free Electron Model, commonly referred to as the Sommerfeld model, incorporated some of the newly discovered laws of quantum

mechanics. It correctly predicts properties that the Drude Model does not, including the temperature dependence of resistivity.

The Sommerfeld model no longer treats the free electrons as classical particles, but rather as quantum mechanical fermions that must obey both the Schrödinger equation and the Pauli Exclusion Principle. Surprisingly, little changes with the adoption of the Sommerfeld model. This is primarily due to the fact that the electrons' wavelengths are tiny compared to the lattice spacing of materials, which is on the order of an angstrom. However, the  $\tau$  in the Sommerfeld model is now split into two components, a temperature dependent and a temperature independent term. The temperature dependent term arises from collisions between the electrons and quantized thermal excitations of the crystal lattice, known as phonons, while the temperature independent term arises from collisions with lattice impurities.

Therefore, the time between collisions is,

$$\frac{1}{\tau} = \frac{1}{\tau} + \frac{1}{\tau_o}, \quad (1.6)$$

where  $\tau_o$  is independent of temperature, and thus Eqn.(1.5) becomes,

$$\rho = \frac{m_e}{ne^2\tau} + \frac{m_e}{ne^2\tau_o} = \rho_i(T) + \rho_o, \quad (1.7)$$

where  $\rho_i$  is known as the ideal resistivity and  $\rho_o$  is the residual resistivity. This separation into ideal and residual resistivity is known as Matthieson's Rule. The residual resistivity is typically measured at the boiling point of helium, 4.2K. At temperatures this low, scattering of electrons by lattice impurities is greater than the scattering by phonons. The temperature where this transition occurs indicates the purity of the sample. If a sample is of high purity, the residual resistivity will take over at a lower temperature.

The Sommerfeld model works well and correctly predicts most fundamental properties. However, there are some areas where even this model fails. For instance, it cannot describe why some materials behave as insulators while others behave as conductors, nor does it predict positive charge carriers [9]. Fortunately, because we are working with metals and the sign of the charge carriers does not affect our measurements, the Sommerfeld model is satisfactory for our purposes.

Resistivity is an important and useful parameter to measure. It is an intrinsic property of a material and is thus independent of the size and shape of a conductor. Also, when measured with high precision, resistivity can be used as an indication of the purity or chemical composition of a substance. The standard procedure for measuring resistivity is a four probe measurement. This method involves using direct electrical connections in the form of solder joints to apply a current to a sample while simultaneously measuring the voltage drop across it, giving a measurement of the electrical resistance. If the dimensions of the sample are known, this resistance measurement can be used to calculate the resistivity.

The eddy current method, first proposed by Bean et al. in 1959 [1], involves using a solenoid to apply a magnetic field to a conductor. The introduction of the magnetic field induces eddy currents in the conductor that act to oppose the changing field. Once the field has fully penetrated the material and the eddy currents have stopped, the field is then quickly removed, which again causes the eddy currents to flow in order to oppose the change in magnetic flux through the material. These currents decay due to the resistivity of the material and therefore produce a changing magnetic field. Surrounding the conductor with a pickup coil allows us to measure the rate of change of magnetic flux through the material as a voltage. The voltage in the pickup coil decays exponentially at a rate that is proportional to the resistivity of the conductor. Four probe measurements are more common than the eddy current

method. However, the eddy current method tends to be easier and quicker to use than four probe measurements because the apparatus involves simply placing a sample inside the secondary coil. A good comparison of the two methods is given in [2]. Sometimes, difficulty making electrical connections or purity contamination issues preclude electrical connection with the sample. This is when the eddy current method is preferred over four probe measurements.

There are other uses for the eddy current method as well. It is often used as a form of non-destructive testing of conductive materials [12]. It is possible to measure the thickness of thin films of metals by adjusting the oscillation frequency of the field and therefore changing the skin depth. Generating eddy currents to various depths of substances is also used frequently in induction heating of materials.

This chapter has provided a definition of resistivity and established our purpose for studying it. The rest of this thesis is devoted to describing our experiment and the data we have collected, as well as providing a write up for others interested in performing the experiment for themselves.

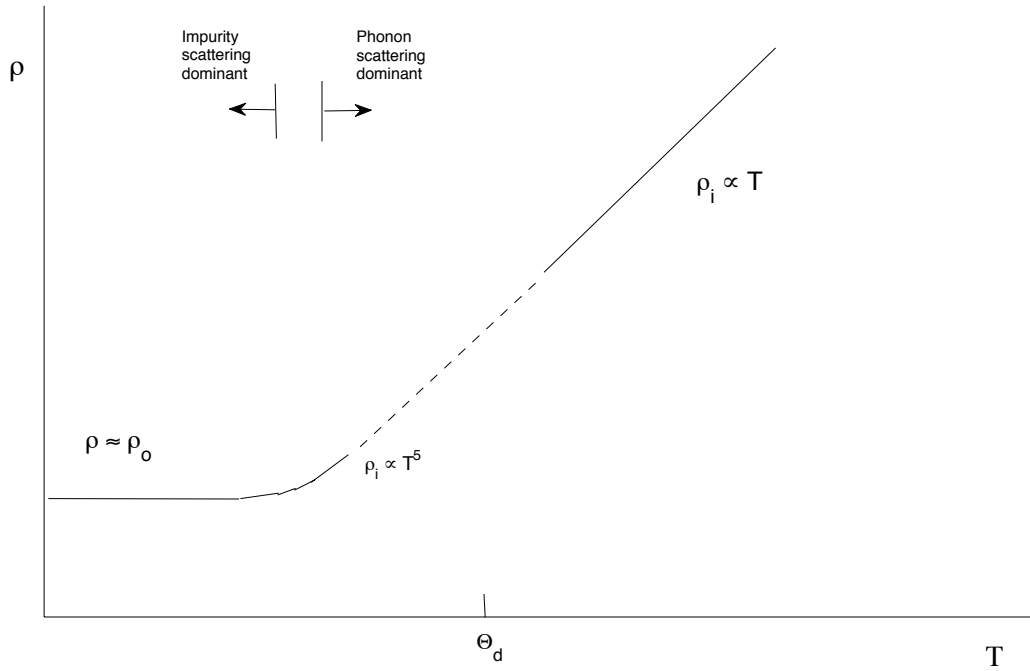


Figure 1.1 The relationship between resistivity and temperature. At temperatures where scattering of the electrons by phonons is dominant, the ideal resistivity varies linearly with temperature. At low temperatures, the residual resistivity due to the scattering of electrons by lattice impurities is dominant and the resistivity is independent of temperature. When neither term is dominant, the dependence is more complicated and is proportional to  $T^5$ . The purity of the sample is indicated by the temperature at which the residual resistivity takes over. For the materials and temperature range we have studied, we remain in the linear region of the curve. This diagram has been adapted from Fig. 3.10 *Solid State Physics* [9].

# Chapter 2

## Experiment

### 2.1 Theory

We turn now to a description of how our experimental setup allows us to measure resistivity. As seen in Fig. 2.2, our apparatus consists of a primary coil for creating the initial magnetic field, and a secondary coil for picking up the changing field due to the decay of the eddy currents in the material. In the absence of the field of the primary coil, the EMF generated in the secondary coil is proportional to the time rate of change of magnetic flux through the material. Thus we need to solve for the form of  $\vec{B}$  using it's derivative, which can be obtained using manipulations of Maxwell's equations. We begin with Ampère's Law

$$\nabla \times \vec{B} = \mu_o \sigma \vec{E}, \quad (2.1)$$

where  $\sigma \vec{E}$  has been substituted in for  $\vec{J}$  and we have ignored displacement currents, which are small. If we take the curl of both sides of this equation and substitute  $\sigma = 1/\rho$ , we obtain

$$\nabla \times (\nabla \times \vec{B}) = \frac{\mu_o}{\rho} (\nabla \times \vec{E}). \quad (2.2)$$

Using Faraday's Law,

$$\nabla \times \vec{E} = -\frac{\partial \vec{B}}{\partial t} \quad (2.3)$$

and substituting into Eqn. [2.2], we get

$$-\nabla^2 \vec{B} = -\frac{\mu_o}{\rho} \frac{\partial \vec{B}}{\partial t}, \quad (2.4)$$

Multiplying the constants, switching to  $\mu$  in the material rather than  $\mu_o$ , and canceling the negative signs, we have

$$\kappa \nabla^2 \vec{B} = \frac{\partial \vec{B}}{\partial t}, \quad (2.5)$$

where  $\kappa = \frac{10^9 \rho}{4\pi\mu}$ . This gives us three equations for  $\vec{B}$  in cylindrical coordinates:  $B_r$ ,  $B_\phi$ , and  $B_z$ . However, the fields from the decaying eddy currents are only in the  $\hat{\phi}$  direction, and those fields depend solely on  $r$  and  $t$ . Using the fact that only the radial derivatives of  $\nabla^2$  will return terms when acting on  $B_\phi(r,t)$ , we have

$$\nabla^2 B = \frac{1}{r} \frac{\partial}{\partial r} \left( r \frac{\partial B}{\partial r} \right), \quad (2.6)$$

where we are now calling  $B_\phi(r,t)$  simply  $B$ . Substituting Eqn.[2.6] into Eqn.[2.5] for  $\nabla^2 B$  we obtain, with some simplification,

$$\frac{\partial B}{\partial t} = \kappa \left[ \frac{\partial^2 B}{\partial r^2} + \frac{1}{r} \frac{\partial B}{\partial r} \right]. \quad (2.7)$$

This is the differential equation we need to solve for  $B$ . We have the following boundary conditions:

$$\begin{aligned} 0 < r < R \\ B(r=0) &= 0 \\ B(r=R) &= 0 \\ B(0 < r < R, t=0) &= f(r), \end{aligned} \quad (2.8)$$

where  $R$  is the radius of the cylindrical conductor. The magnetic field just outside the rod is zero and, in order that the magnetic field be continuous across the boundary, the magnetic field at the surface must also be zero. This implies there are no surface currents to cause a change in  $B$  across the boundary.

This differential equation is often seen in heat diffusion problems and there exist many texts dedicated to solutions of these types of equations [3] [4]. The first step is to assume a separable solution, with exponential time behavior:

$$B(r, t) = U(r)T(t) = U(r)e^{-\kappa\alpha^2 t}. \quad (2.9)$$

When we plug this form of the solution into the differential equation, Eqn.[2.7], we get

$$U[-\kappa\alpha^2]e^{-\kappa\alpha^2 t} = \kappa \left[ \frac{\partial^2 U}{\partial r^2} e^{-\kappa\alpha^2 t} + \frac{1}{r} \frac{\partial U}{\partial r} e^{-\kappa\alpha^2 t} \right]. \quad (2.10)$$

Dividing through by the similar terms, we are left with

$$\frac{\partial^2 U}{\partial r^2} + \frac{1}{r} \frac{\partial U}{\partial r} + \alpha^2 U = 0, \quad (2.11)$$

which is a Bessel Equation of order zero. However, the equation becomes easier to work with if we divide by  $\alpha^2$  and make the change of variables,  $x = \alpha r$ . Our equation then becomes,

$$\frac{\partial^2 U}{\partial x^2} + \frac{1}{x} \frac{\partial U}{\partial x} + U = 0. \quad (2.12)$$

The solution to a zero order bessel equation can be found in many sources [11] and is a combination of Bessel functions of the first and second kind,  $J$  and  $N$  respectively.

$$U(x) = AJ_0(x) + BN_0(x) \quad (2.13)$$

It is at this step that we can eliminate functions of the second kind due to the boundary condition  $U(x = 0) = 0$  and  $N_0$  tends toward infinity at  $x = 0$ .

The general solution to our equation is now an infinite series,

$$B = \sum_{n=1}^{\infty} A_n J_0(\alpha_n r) e^{-\kappa \alpha_n^2 t}. \quad (2.14)$$

To satisfy the boundary condition that  $B = 0$  at  $r = R$ ,  $\alpha$  must be a root of the Bessel equation  $J_0(\alpha R) = 0$ . These roots can be found in Bessel function tables and various mathematical reference texts. I list the first few here due to their importance to our work,

$$\lambda_1 = 2.405, \quad \lambda_2 = 5.520, \quad \lambda_3 = 8.654. \quad (2.15)$$

Solving for the roots in terms of  $\alpha$

$$\alpha_n = \frac{\lambda_n}{R}. \quad (2.16)$$

Therefore, the magnetic field takes the final form,

$$B(r, t) = \sum_{n=1}^{\infty} A_n J_0\left(\frac{\lambda_n r}{R}\right) e^{-\kappa \lambda_n^2 / R^2 t}. \quad (2.17)$$

Now that we have the functional form of  $B$ , we can use this to obtain a more useful form of the voltage generated in the pickup coil. The voltage induced in the pickup coil is proportional to the time rate of change of magnetic flux through the rod placed inside the pickup coil. It is easiest to solve for the flux first and then take the time derivative to solve for the voltage. The flux is acquired by integrating the magnetic field over the cross sectional area of the rod,

$$\Phi = \int_0^R B \cdot da = \int_0^R B \cdot 2\pi r dr, \quad (2.18)$$

where  $da$  is given for cylindrical coordinates. Substituting the form of  $B$  given by Eqn. [2.17], removing the constant terms from the integral, and simplifying the exponential

terms with the substitution

$$t_{En} = \frac{1}{\kappa} \left( \frac{R}{\lambda_n} \right)^2 = \frac{4\pi\mu}{10^9\rho} \frac{R^2}{\lambda_n^2}, \quad (2.19)$$

we obtain,

$$\begin{aligned} \Phi &= 2\pi \sum_{n=1}^{\infty} A_n e^{-t/t_{En}} \int_0^R r J_0\left(\frac{\lambda_n r}{R}\right) dr \\ &= 2\pi \sum_{n=1}^{\infty} A_n e^{-t/t_{En}} \frac{R}{\lambda_n} J_1(\lambda_n). \end{aligned} \quad (2.20)$$

The next step is to take the time derivative and simplify,

$$\frac{d\Phi}{dt} = 2\pi\kappa \sum_{n=0}^{\infty} A_n \frac{\lambda_n}{R} J_1(\lambda_n) e^{-t/t_{En}}. \quad (2.21)$$

The voltage signal induced in the pickup coil is proportional to this change in flux

$$V(t) = N \frac{d\Phi}{dt} \quad (2.22)$$

where  $N$  is the number of turns in the pickup coil. However, for longer times, the exponentials with higher order roots have essentially died out and we can approximate the signal as a single exponential with the root  $\alpha_1$ ,

$$V(t) = 2\pi N A_1 \kappa \frac{\lambda_1}{R} J_1(\lambda_1) e^{-t/t_E}. \quad (2.23)$$

Also, only the exponential term depends on time and we can consolidate the remaining terms into a constant,  $V_0$ ,

$$V(t) = V_0 e^{-t/t_E}. \quad (2.24)$$

where

$$t_E = 2.17 \times 10^{-9} \frac{R^2}{\rho}. \quad (2.25)$$

Taking the natural log of both sides of this equation, we obtain

$$\ln[V(t)] = \ln(V_0) - \frac{1}{t_E} t, \quad (2.26)$$

which is simply the equation of a line with a slope  $1/t_E$  (See Fig. 2.1). Solving Eqn.[2.25] for  $\rho$ ,

$$\rho = 2.17 \times 10^{-9} \frac{R^2}{t_E} \quad (2.27)$$

we arrive at an equation we can use to measure the resistivity of cylindrical conductors.

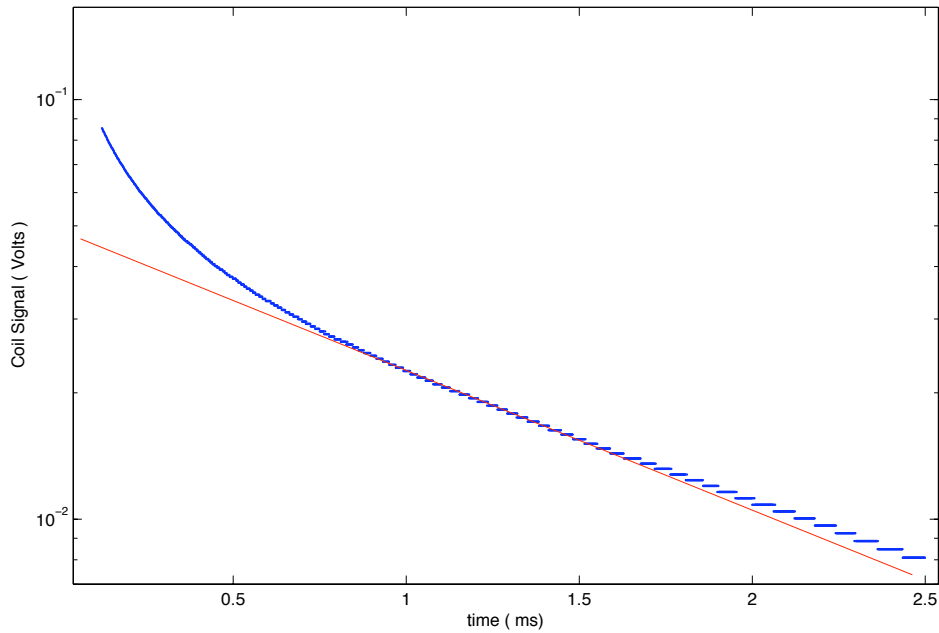


Figure 2.1 The pickup coil signal as a function of time that we use to measure the resistivity. Also shown is a linear fit of a select part of the data, from about 1 to 1.5 ms. At earlier times the signal is not described by a pure exponential and at later times we reach the resolution of the oscilloscope. These data are for a 1/2" copper rod at  $T = 130\text{K}$ .

## 2.2 Construction of Apparatus

The first step in the process was to design and construct both a primary and secondary coil. The primary coil, used to create the magnetic field, was quite simple to design. We carefully wrapped AWG 18 copper wire around a cylindrical piece of PVC 1.9 inches in diameter, and secured it using VGE-7031 insulating varnish. With currents as high as 2A, the 18 gauge wire was necessary in order to keep the resistance of the coil low to minimize heating. With the approximation that we have an infinite solenoid, the field at the center of the solenoid is given by [5]

$$B = \mu_0 n I, \quad (2.28)$$

where  $n$  is the number of turns per unit length and  $I$  is the current in the wire. We determined by counting that the number of turns per unit length for the primary coil were 10 turns per cm. Therefore, with currents ranging from 1.5 to 2 A, the field at the center is around 2 Gauss. Upon testing the coil, we determined the field was large enough to give us a measurable signal.

This primary solenoid is driven by a Kenwood *PR36 - 3* regulated dc power supply. However, because the changing magnetic flux we measure with the pickup coil must be a result of the decay of the eddy currents alone, we need a way to reduce the primary field to zero very quickly, on the order of microseconds. The best way to accomplish this is to drive the primary solenoid through a transistor that can be switched off and on by a function generator (see Fig. 2.3). We have used an IRLZ24N HEXFET, due to its fast switching speeds, low gate turn on voltage, and ability to handle the amount of power we would be delivering from the current source. The diodes between the pickup coil and the oscilloscope protect it from any voltage spikes resulting from the very rapid change in magnetic flux. The square wave is symmetric and has a period  $\tau$  such that  $\tau/2$  is greater than the lifetime of the signal, which is

on the order of 2 ms. We used a frequency of 120 Hz corresponding to a period of 8 ms. The square wave is sent to the scope to verify the signal and to trigger the oscilloscope to read the voltage from the pickup coil when the square wave is low. The ground for the toggling circuit is kept separate from the ground for the pickup circuit.

Construction of the pickup coil proved to be a much more difficult task. We did not want to amplify the signal and thus the coil needed enough turns to produce a measurable voltage with the oscilloscope we were using. Our original design consisted of AWG 24 copper wire wrapped neatly around a slightly smaller piece of PVC than the primary coil. Upon using this coil, we discovered that there were oscillations present in the signal due to the inductance and capacitance of the coils. These oscillations die out due to the resistance of the coil. We needed the oscillations to reduce to zero in a much shorter time than the lifetime of our signal, which for aluminum and copper was on the order of 500  $\mu\text{s}$ . We determined that it was necessary to reduce both the inductance and capacitance of the coil. The textbook that originally provided us with the idea for the experiment [6] had mentioned criss-crossing the windings of the pickup coil in order to reduce the intrinsic capacitance. We also decided to use smaller diameter wires with AWG 40 wire. Our second pickup coil worked significantly better than the first, however, the oscillations still lasted too long and the new design was also quite fragile. Our third design included fewer turns, criss-crossed windings, but slightly larger diameter wire to be more durable. This coil performed well with the oscillations dying out in about 80  $\mu\text{s}$ . However, the lifetime of the voltage signal is much shorter for brass due to the higher resistivity when compared to aluminum and copper. Therefore, we sought to reduce the lifetime of the LC oscillations even further with a fourth and final coil design. This fourth coil used AWG 34 wire, criss-crossed windings, and about the same number of turns as the third coil. The lifetime of the

oscillations in coil 4 is  $40 \mu\text{s}$  (Fig. 2.4). This is short enough that it does not affect our measurements.

### 2.2.1 Adapted for Temperature-Dependent Measurements

Our main goal for this experiment was to measure the temperature dependence of resistivity down to the boiling point of Nitrogen. In order to do this, we first needed a way to measure the temperature of our samples. We chose DT-471 silicon diode thermometers built by LakeShore Cryotronics, Inc.. These diodes were accurate enough for our measurements and involved no electrical contact to the sample (Refer to Fig. 2.5).

We needed to be sure that the samples warmed up uniformly, so that the temperature of the rods was about the same at the center as it was on the surface. To make this measurement, we purchased two of the diodes and placed one on the surface and the other in the center of the rod. For these initial measurements, we used a Neocera *LTC-21* temperature controller to monitor the temperatures of the two diodes. The data were recorded in a text file and imported into MATLAB for analysis.

We set out with the hope that the two temperatures would differ by no more than 2K at any point. We first ran the experiment with no insulation on a half inch diameter aluminum rod. As expected, the rod warmed up rather quickly and the temperatures differed by almost 10K at some points. We then tried various types of insulation with the constraint of restricting the size of the insulated rod to fit into the pickup coil. After various trials, we settled on a thin layer of teflon tape, a layer of mylar polyester film, and then another few layers of teflon tape. This insulation worked well and allowed us to fit the rod inside the pickup coil. We compare the warm up with and without insulation in Fig. 2.6. Unfortunately, we had removed the diode mounted at the center of the rod when we recorded the warmup with

insulation. However, if we consider the heating in the rod—represented by the slope of the temperature vs. time graph—to be proportional to the temperature difference between the surface and the center, we can match the slope at a point on both graphs and use the corresponding temperature difference from the uninsulated data. Using this model, we estimate that the temperature difference between the center and surface of the insulated rod vary by no more than 5K at any point below 150K and by no more than 3K above 150K. At any temperature above 200K, the difference oscillated just above and below 1K.

Unfortunately, the temperature controller that we used to record the warm up data was not available for permanent use with this experiment. Therefore, temperature measurements were made using a Keithley 224 current source to provide  $10\mu\text{A}$  of current to the diode and a Fluke 29 multimeter to measure the voltage across the diode. Lakeshore provided us with the calibration curve for the diodes and, using this graph, we can convert the voltage on the voltmeter to the temperature of the diode. A good project for future students would be to add a feature to the LabVIEW program to read the voltmeter, convert the voltage to a temperature, and store that temperature with the resistivity data all in one file.

## 2.3 Data Acquisition

Acquiring the data is a time intensive task that requires about four hours from start to finish. The resistivity measurement is very sensitive to which part of the signal is used. The LabVIEW program sends the voltage and time data that is displayed on the oscilloscope screen to a text file on the computer. It is best to maximize the desired segment of the signal on the screen by moving the zero level of the oscilloscope to the bottom of the screen and using the smallest vertical and horizontal scales possible on

the oscilloscope. If the data is recorded too early, the signal will not be represented by a pure exponential. If it is recorded too late, the voltages are small and the resolution of the oscilloscope is reached. Also, we have provided a graph of the natural log of the voltage signal on the front panel of our LabVIEW program. Using this, we can take data and ensure that the natural log gives us a straight line. With some practice, it becomes clear to the user which part of the signal consists results in the best data. The signal changes as the rod warms up and this occurs quickly at low temperatures. Therefore, the time and voltage scales must be adjusted while taking the data.

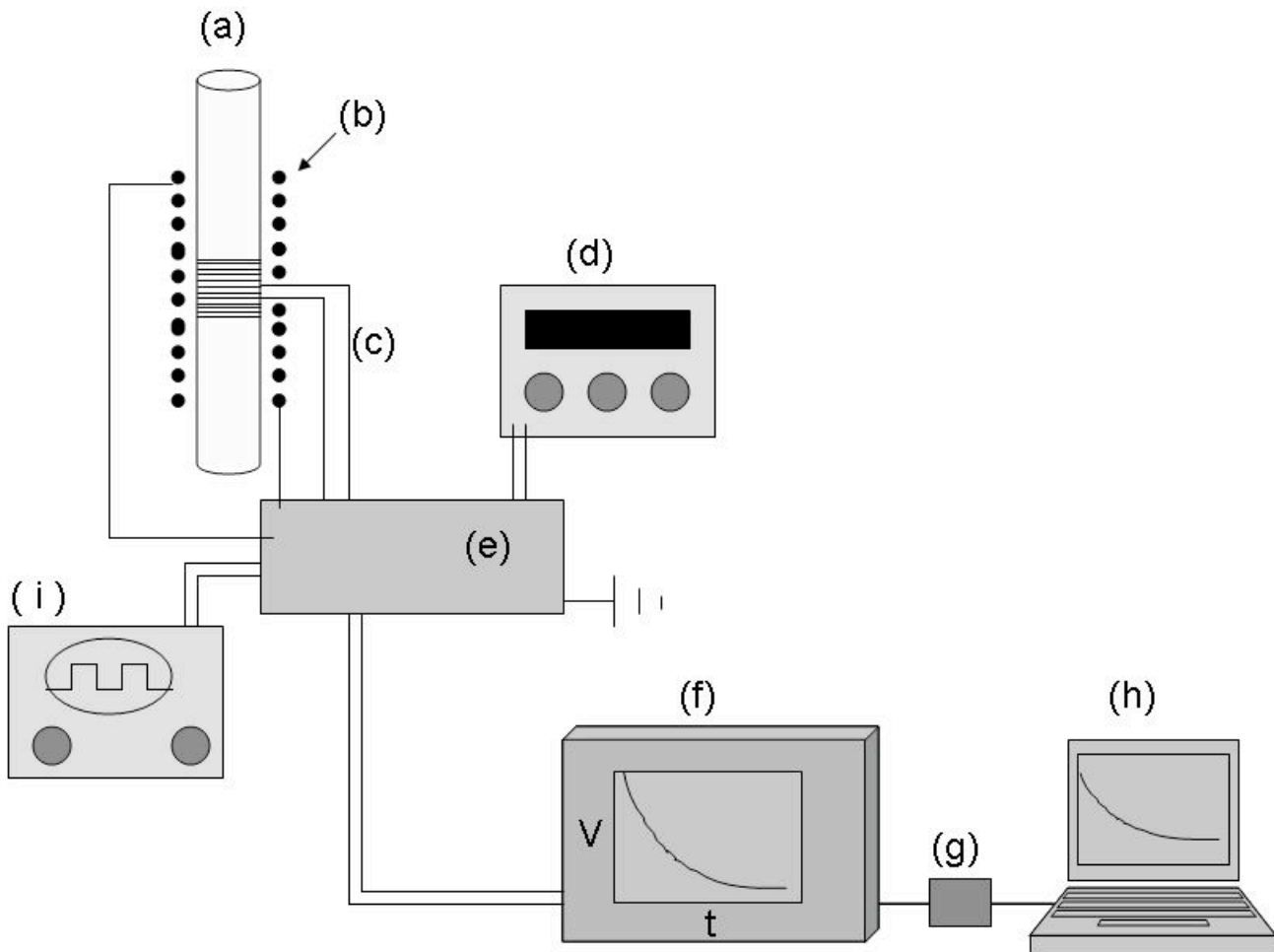


Figure 2.2 This is a diagram of our experimental setup including all the important components with the exception of the circuit diagram which appears in Fig. 2.3: The cylindrical conductor (a) is surrounded by the primary coil (b) which applies the magnetic field. The primary coil is powered by a 3A power supply (d) via a transistor in the electronic circuit (e). The transistor, and thus the magnetic field, is switched on and off by a square wave generator (i). The leads from the pickup coil (c) go directly to the circuit which connects to the digital oscilloscope (f). The oscilloscope sends the signal to the computer (h) via a GPIB-USB interface(g) and National Instruments LabVIEW.

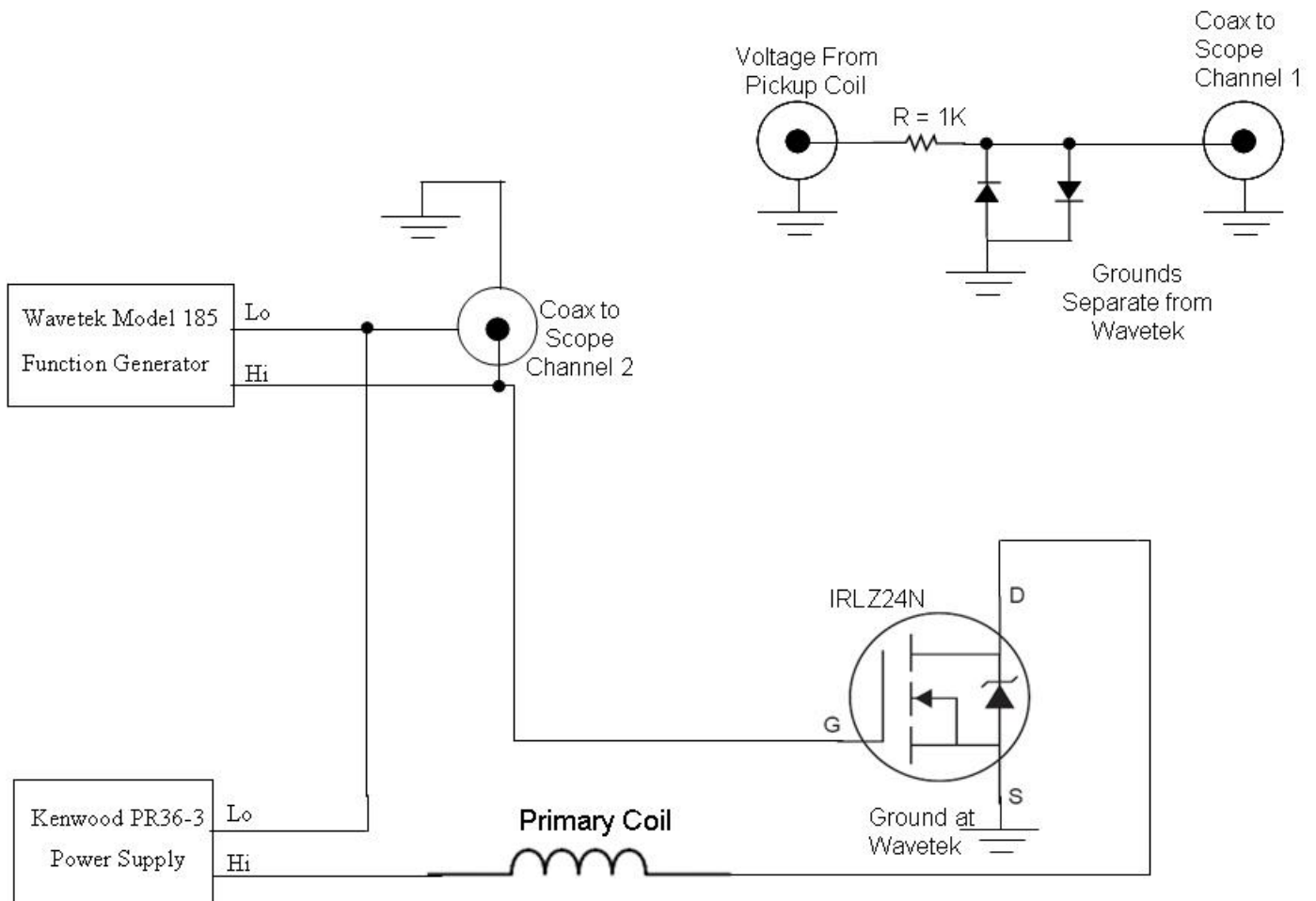


Figure 2.3 Shown here is the circuit used to toggle the magnetic field as well as deliver the signal to the oscilloscope. The transistor is toggled by the function generator. The pickup coil is placed inside the primary coil and the signal is sent to the oscilloscope. The diodes clamp the input signal between  $\pm 0.6V$  so as to protect the oscilloscope from the large voltages that may be induced due to the rapid change in magnetic flux when the field is turned off. The square wave that toggles the coil is sent to the oscilloscope to trigger it to read the voltage from the pickup coil when the square wave is low.

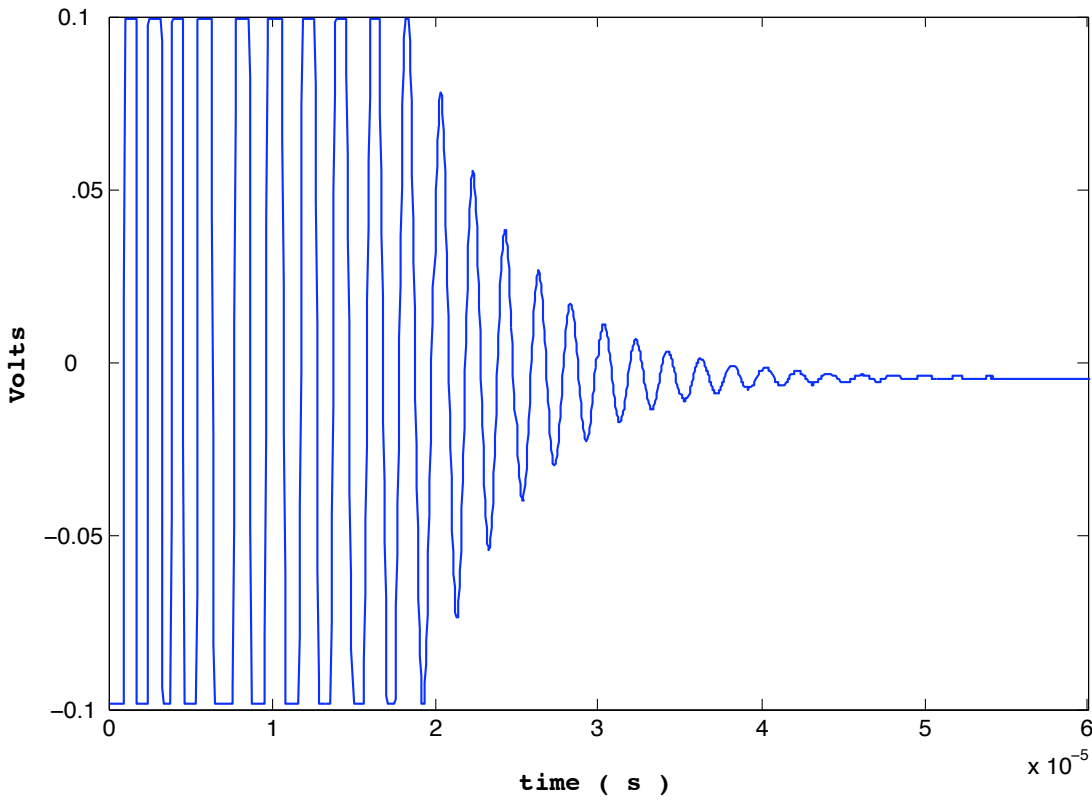


Figure 2.4 The LC oscillations for coil 4. These oscillations decay to zero quick enough to not affect our measurements. We worked to reduce the inductance and capacitance of the coil to reduce the effect of the oscillations on the voltage signal.

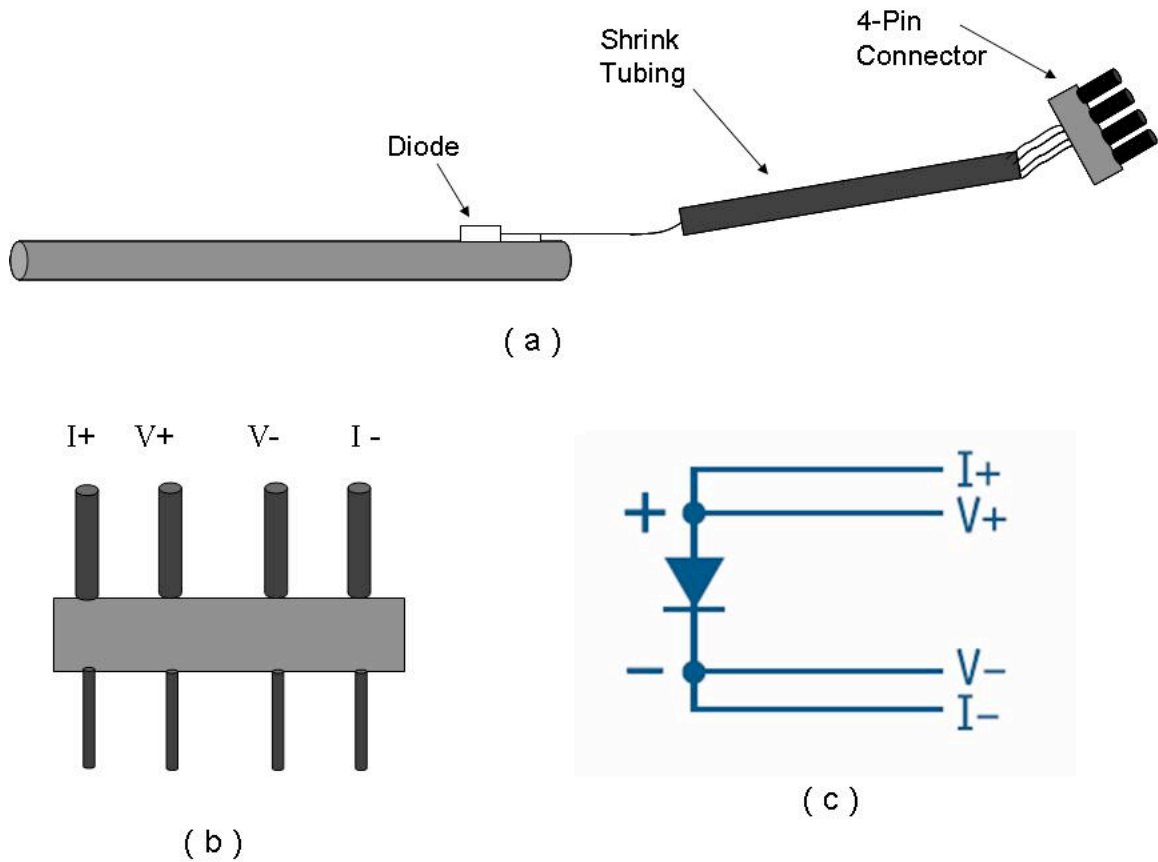


Figure 2.5 (a) The diode thermometers are mounted on the surface of the rod away from the section enclosed by the pickup coil. The teflon tape insulation holds the thermometer firmly against the surface. (b) The diode's leads are soldered to a four pin connector. This increases the durability of the setup and makes it easier to deliver the current and read the voltage. (c) Copper wires are soldered to the diode in a four lead measurement setup.

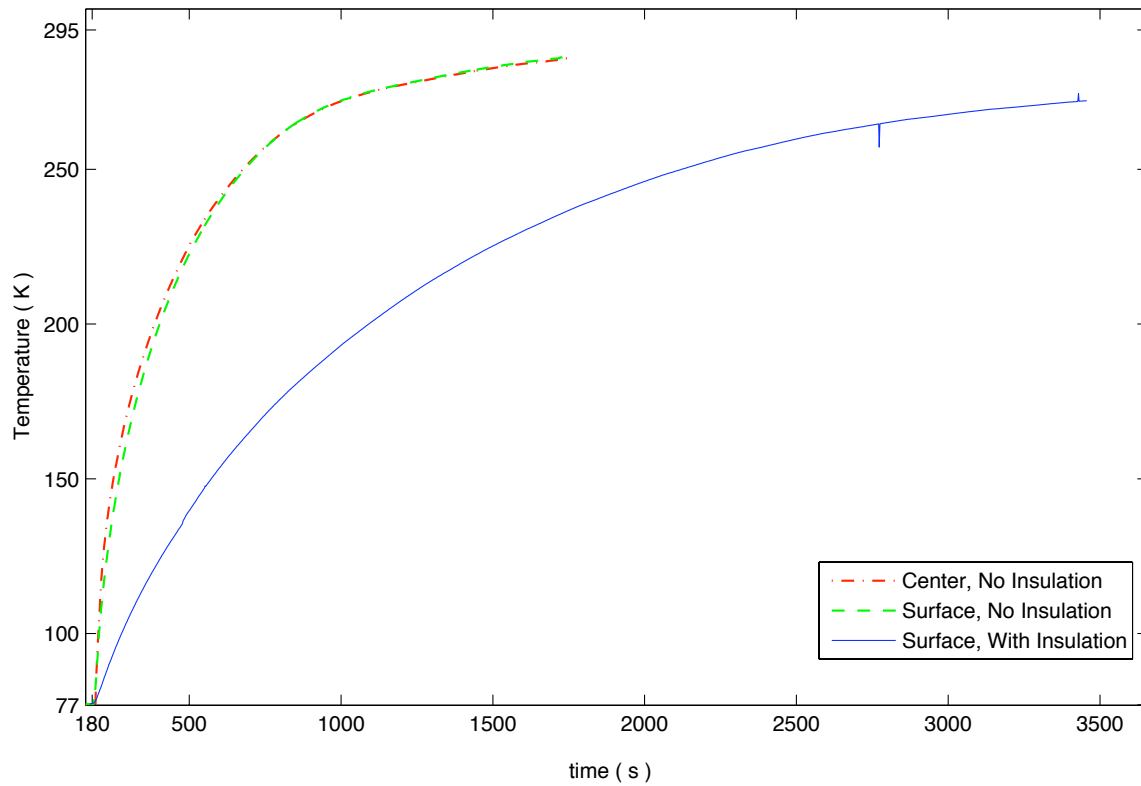


Figure 2.6 Here we compare the warmup of the insulated rod to the uninsulated case. Unfortunately, the thermometer at the center of the insulated rod was removed before we performed the experiment. However, using a simple model for heat diffusion described in the text, we estimate that the temperature difference between the surface and center did not exceed 5K at any point. Also, at temperatures above 150K, the difference never exceeded 3K.

# Chapter 3

## Results

We wanted to be sure our experiment worked at room temperatures before we adapted it for temperature dependent measurements. We decided to measure the resistivity of a pure metal and an alloy. The pure metal would allow us to compare our results with previous work. However, resistivity data for alloys depends greatly on the composition of the alloy used. Therefore, if the chemical composition of the alloy used does not exactly match that of references that can be found, comparing the experimentally determined values to accepted values can be difficult. The pure metal serves to show that our experiment is capable of obtaining data that agree well with previous work while the alloy is to test our experiment with a metal that may not be listed in very many sources.

We have used 99.994% pure copper and the common 6061 aluminum alloy with a composition of 1% Mg 0.6% Si. Table 1 contains the values obtained for the room temperature measurements along with the accepted value for pure copper. We managed to find a source that listed the resistivity for 6061 aluminum as  $3.25 (\times 10^{-8} \Omega \cdot m)$  [8]. However, the chemical composition listed was that of 0.5% Mg and 0.5% Si. Given our higher percentage of both Mg and Si, it seems logical that our value for resis-

tivity be higher. The data for copper are very self consistent. The upward trend with increasing radius could be due to the shorter time scale and smaller voltages for the signals of smaller rods. However, the resistivities certainly scale well for the different radii. The signals from the quarter inch rods were the hardest to obtain due to the rather quick decay. The half inch rods returned the best data due to the higher voltages and longer decay times. With the longer decay times, the linear fit will improve because the approximation of a single exponential is more accurate for longer times. Our data for the aluminum also follow the upward trend with increasing radius. These data are harder to compare to accepted values due to the dearth of sources listing resistivity for the chemical composition we used. However, the accuracy of our copper measurement leads us to trust that our aluminum measurement is just as accurate. The shorter signal length due to higher resistivity in the aluminum rods could account for the larger discrepancy between the different size rods than is present in the copper measurements. This discrepancy could also arise from the fact that the different rods could have slightly different chemical composition. If we were to perform the experiment again, we would use the same aluminum rod for all the measurements and use a lathe to reduce the radius of the rod. This would insure that the chemical composition remained constant for our measurements.

Once we were certain that we were obtaining reasonable numbers, we moved on to temperature dependent measurements. We cooled the rods with liquid nitrogen and recorded the signal from the oscilloscope as the rods warmed up to room temperature. These data are shown in Figs. 3.1 and 3.2 and certainly constitute a good linear fit that agree well with the temperature dependences listed in [7]. We used the half inch rods because, as previously stated, that allowed us to acquire the best signal. Also, the longer decay times at lower temperatures again assists our approximation

Table 1. Experimentally determined resistivities at 293K compared to accepted value. The accepted value for copper is taken from the National Bureau of Standards Survey of Electrical Resistivity [7].

Material	Diameter(In.)	$\rho(\times 10^{-8}\Omega \cdot m)$	Accepted Value
Pure Copper	1/2	1.69	1.68
–	3/8	1.68	–
–	1/4	1.66	–
6061 Aluminum	1/2	3.47	3.25 *see text
–	3/8	3.34	–
–	1/4	3.32	–

Table 2. Our final values listed with the uncertainties in our measurements. We have included the National Bureau of Standards data for copper to compare our measurements to previous work.

Material	$\rho(\times 10^{-8}\Omega \cdot m)$	$\rho_{NBS}$
Pure Copper	$1.69 \pm 0.02$	$1.68 \pm 0.01$
6061 Aluminum	$3.47 \pm 0.02$	* see text

of a single exponential. Therefore, the segment of signal used to obtain a linear fit increases at lower temperatures

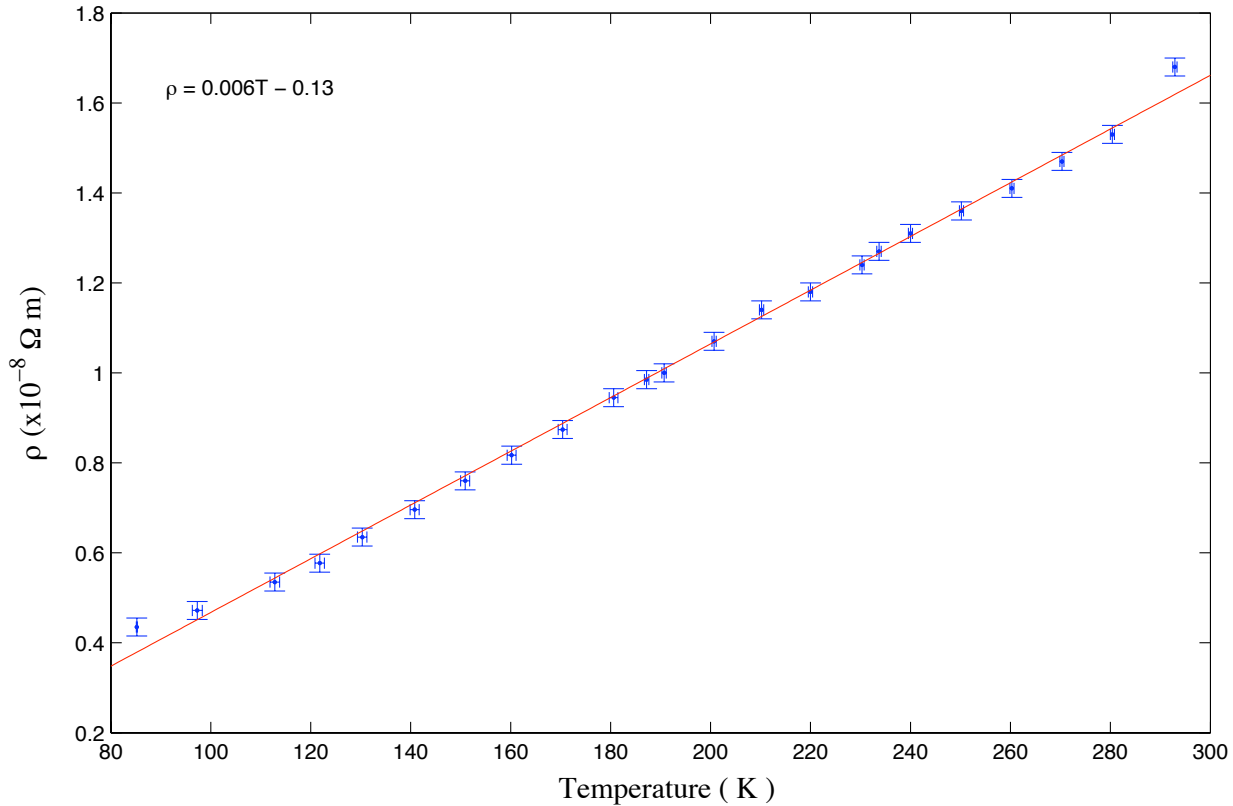


Figure 3.1 The linear temperature dependence of resistivity for a 1/2" copper rod. We cooled the rod in liquid nitrogen and recorded the signal from the pickup coil as the rod warmed up. Data points were taken about 10K apart. Despite the room temperature measurement being slightly higher than is predicted by the linear fit, the measurement of  $1.68 \pm 0.02(\times 10^{-8} \Omega \cdot m)$  compares well with the accepted value of  $1.678(\times 10^{-8} \Omega \cdot m)$  which is within our range of uncertainty.

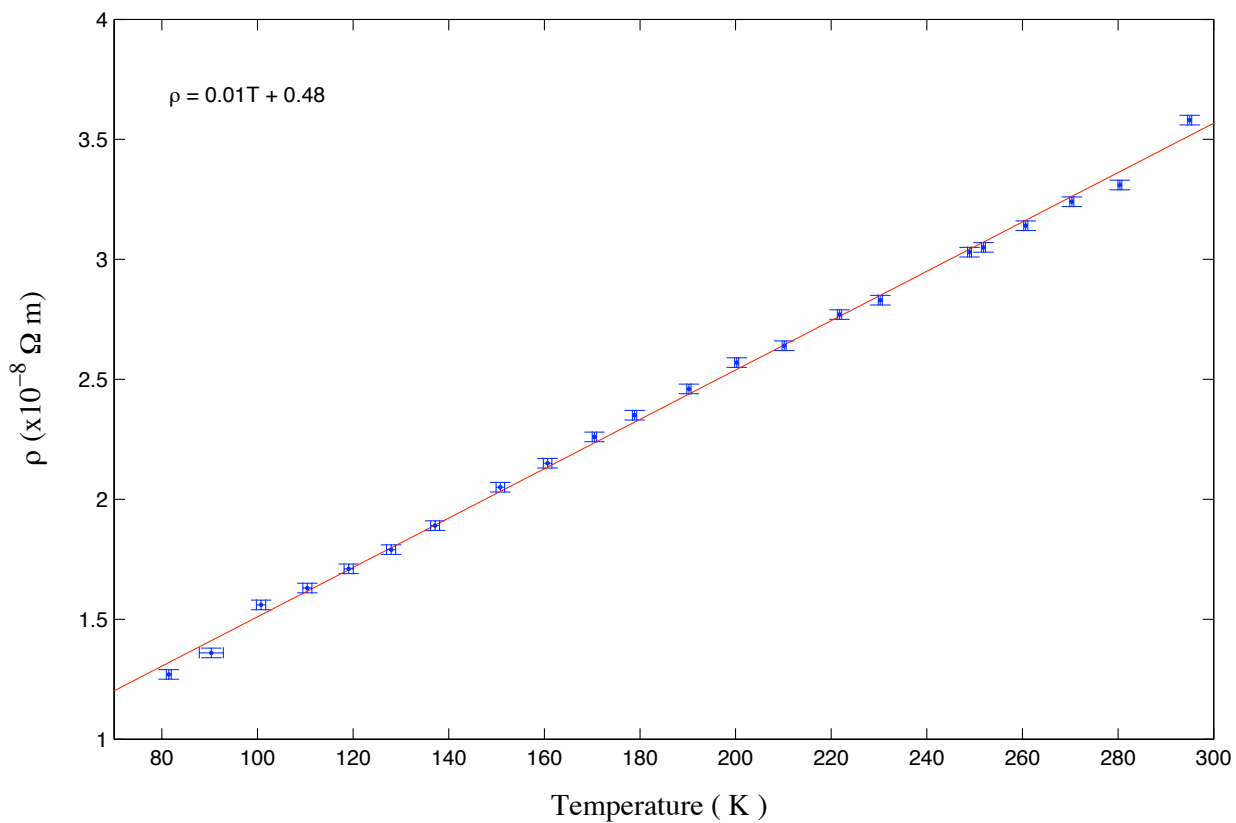


Figure 3.2 Results for a 1/2" 6061 aluminum rod. The resistivity varies linearly with temperature and again the room temperature measurement is higher than is predicted by the linear fit.



# Chapter 4

## Future Work

Comparing our results with previous work, we are satisfied with the outcome of our experiment. While we are satisfied, there are certainly aspects that can be improved. The first step would be to enhance the LabVIEW program and have it read the diode voltage as well as the signal from the oscilloscope. This would speed up the process and would reduce the probability of making a mistake when dealing with multiple text files. We often reached the resolution of the oscilloscope with our measurements. To avoid this, a 12 or 16 bit analog to digital converter could be implemented to deliver the data to a computer.

To measure residual resistivity, it is necessary to reach the boiling point of helium, 4.2K. Performing experiments at temperatures this low requires advanced cryogenic equipment. The coils would need to be contained in a vacuum dewar and would need to be built to withstand such a low temperature environment. It is certainly within the capabilities of the department to make these modifications.

After some refinement, we intend this experiment to be performed by undergraduate students in the advanced laboratory classes at Ithaca. This class is usually taken during students' junior year and requires them to perform experiments and write up

their results in a scientific paper. This experiment will fit in well with the curriculum because it requires students to draw on various skills such as computer programming, statistical data analysis, and working with an oscilloscope. It also serves as an introduction to solid state physics and a refresher on some electromagnetic theory.

# Bibliography

- [1] C.P.Bean et al., "Eddy-Current Method for Measuring the Resistivity of Metals,"  
Journal of Appl. Phys. **30**, 12, June 29, 1959
- [2] A.B. Kos and F.R. Fickett, "Improved Eddy-Current Decay Method For Resistivity Characterization", IEEE Transactions on Magnetics, **30**, No. 6, November 1994
- [3] H.S. Carslaw and J.C. Jaeger, *Conduction of Heat in Solids*, 2nd ed. (Oxford University Press, London, 1959)
- [4] B. Wwedensky, Annalen der Physik **369**, 609-620 (1921)
- [5] D.J.Griffiths, *Introduction to Electrodynamics*, 3rd ed. (Prentice-Hall, New Jersey, 1999)
- [6] A.C. Melissinos, *Experiments in Modern Physics*, 2nd ed. (Academic Press, 2003)
- [7] L.A. Hall, "Survey of Electrical Resistivity Measurements on 16 Pure Metals in the Temperature Range 0 to 273K", NBS Technical Note 365, U.S. Superintendent of Documents, 1968
- [8] W.F. Gale *ed.* and T.C. Totemeier *ed.*, *Smithells Metals Reference Book*, 8th ed. (Elsevier Butterworth-Heinemann, Boston, 2004)

- [9] J.R. Hook and H.E. Hall, *Solid State Physics*, 2nd ed. (Wiley, 1995)
- [10] Jeremy Bernstein, Paul M. Fishbane, and Stephen Gasiorowicz *Modern Physics*, 1st ed. (Prentice-Hall, New Jersey, 2000)
- [11] M. L. Boas, *Mathematical Methods in the Physical Sciences*, 3rd ed. (Wiley, New York, 2005)
- [12] Non-Destructive Testing Resource Center, “Basic Principles of Eddy Current Inspection” <http://www.ndt-ed.org/EducationResources/CommunityCollege/EddyCurrents/Introduction/IntroductiontoET.htm> (Accessed March 1, 2009)